Journal of Molecular Graphics and Modelling 121 (2023) 108431

Contents lists available at ScienceDirect

Journal of Molecular Graphics and Modelling

journal homepage: www.elsevier.com/locate/jmgm

A modified bonded model approach for molecular dynamics simulations of New Delhi Metallo-β-lactamase

Amani A. Eshtiwi [1], Dan L. Rathbone [*]

College of Health and Life Sciences, Aston University, Birmingham, B4 7ET, UK

ARTICLE INFO

Keywords:
Molecular dynamics (MD)
Bonded model
Metal centre parameter builder (MCPB)
New Delhi metallo-β-lactamase 1 (NDM-1)
β-lactams
Metalloproteins

ABSTRACT

Modelling metalloproteins using the classical force fields is challenging. Several methods have been devised to model metalloproteins in force fields. Of these methods, the bonded model, combined with Restrained Electrostatic Potential (RESP) charge fitting, proved its superiority. The latter method was facilitated by the development of the python-based Metal Centre Parameter Builder (MCPB.py) AmberTool. However, the standard bonded model method offered by the MCPB.py tool may not be appropriate for validating and refining the binding modes predicted by docking when crystal structures are lacking. That is because the representation of coordination interactions between any bound ligand and metal ions by covalent bonds can hinder the flexibility of the ligand. Therefore, a new modification to the standard bonded model approach is proposed here. Molecular dynamics (MD) simulations based on the new modified bonded model (MBM) approach avoid the bias caused by coordination bonds and, unlike hybrid QM/MM MD, allow for sufficient sampling of the binding mode given the currently available computational power. The MBM MD approach reproduced the studied crystal structure conformations of New Delhi Metallo-β-lactamase 1 (NDM-1). Furthermore, the MBM approach described the binding interactions of intact β-lactams with NDM-1 reasonably, and predicted a non-productive binding mode for the poor NDM-1 substrate aztreonam whilst predicting productive binding modes for known good substrates. This study presents a useful MD method for metallo-β-lactamases and provides better understanding of β-lactam substrates recognition by NDM-1. The proposed MBM approach might also be useful in the investigation of other metal-containing protein targets.

1. Introduction

New Delhi Metallo-β-lactamase 1 (NDM-1) is produced by Gram-negative bacterial strains and has spread worldwide. It utilizes two Zn^{2+} ions to catalyse the hydrolysis of bicyclic β-lactam antibiotics, thus rendering them ineffective. NDM-1 is resistant to the clinically used β-lactamase inhibitors [16], and clinically useful NDM-1 inhibitors are yet to be identified [19].

Indeed, inhibitor discovery may have been impeded by a lack of knowledge of the initial binding modes of β-lactam substrates, since crystal structures of metallo- β-lactamases (MBLs) with intact β-lactams are currently unavailable. Therefore, the computational investigation of NDM-1-substrate complexes is indispensable as it can help in the design of effective mechanism-based NDM-1 inhibitors.

In spite of advanced docking protocols, molecular docking can generate a model of protein-ligand complex with only a limited consideration of protein flexibility. Therefore, classical MD simulations are essential to investigate protein-ligand interactions with full flexibility and to validate the docking pose [7]. However, modelling NDM-1 and other metalloproteins using classical force fields (FFs) is not straightforward owing to the high charges on metal ions, the partially covalent nature of the coordination bonds, and the numerous possible binding modes resulting from the multiple coordination numbers of transition metals [7,9,35].

Several methods have been devised to model metalloproteins in FFs. The non-polarisable models are the most widely used methods to build MM models of metalloproteins because they are simpler and faster than the polarisable models, and can be handled by the common MD

Abbreviations: FF, Force field; MBM, Modified Bonded Model; MD, Molecular Dynamics; MM, Molecular Mechanics; NDM-1, New Delhi Metallo-β-lactamase 1; QM, Quantum mechanical; MBL, Metallo-β-lactamase.

* Corresponding author.
E-mail address: d.l.rathbone@aston.ac.uk (D.L. Rathbone).

[1] On secondment from the Faculty of Pharmacy, Tripoli University, Tripoli, Libya and funded by the Libyan Ministry of Education.

https://doi.org/10.1016/j.jmgm.2023.108431
Received 15 November 2022; Received in revised form 2 February 2023; Accepted 10 February 2023
Available online 17 February 2023

simulation programs [50]. The non-bonded model [24,26] which is the simplest model, the cationic dummy atom model [2] which is also described as the semi-bonded model, and the bonded model [37] are the three categories of the non-polarisable models.

The non-bonded model involves electrostatic and VDW terms. The latter are represented by the 12-6 Lennard-Jones potential which includes Pauli repulsion and induced dipole-induced dipole interactions. This potential is poorly suited for divalent and highly charged metal ions. However, the nonbonded model was improved by the 12-6-4 Lennard-Jones potential developed by Li & Merz [24] by adding a term representing ion-induced dipole interactions. The model also included parameters for monovalent to tetravalent metal ions. Nonetheless, the partial charge of the metal ion in the non-bonded model is identical with its oxidation state. Therefore, this simple model overlooks charge transfer and polarisation effects [24]. In addition, this model can result in a deformed metal coordination geometry and may even fail to keep the metal in the binding site [28].

Pang et al. [36] illustrated the superiority of the cationic dummy atom model to the non-bonded model in maintaining the zinc coordination geometry during MD simulations. In the cationic dummy atom model, which is suitable for tetrahedral zinc coordination, four dummy atoms are linked covalently to zinc in a tetrahedral geometry. The zinc ion is described solely by VDW terms while its charge of +2e is divided equally between the four dummy atoms. The interactions between the dummy atoms and the ligating residues are then represented by electrostatic terms. However, the parametrisation of this model is not straightforward and the model performance depends largely on the charge model used [28].

The bonded model [37] treats the interactions of metal with its ligands as covalent bonds. Thus, it comprises bonded terms (bond, angle, and torsional terms) and non-bonded terms (electrostatic and VDW terms). Therefore, the bonded model guarantees the preservation of the metal coordination geometry during the simulation though at the expense of modelling the ligand exchange processes. Unlike the non-bonded model, the charge on the metal is a non-integer preferably derived from Restrained Electrostatic Potential (RESP) [3] calculations [28]. In addition, parametrisation is carried out for bond and angle terms while torsional and VDW terms are not parametrised as they are considered less significant in metals [37].

Bond and angle parameters are obtained from intensive quantum mechanical calculations using the Seminario method [44] or Z-matrix method on a small model of the metal centre that involves the side chains of coordinating residues capped with methyl groups. Charge calculations are performed on a larger model of the metal centre including the coordinating residues with capped backbones. Charge parametrisation can be performed by including all the atoms of the ligating residues (ChgModA), or by fixing the charges of the backbone heavy atoms (ChgModB), all the backbone atoms (ChgModC), or all the backbone atoms and the beta carbons of the coordinating residues (ChgModD) to the employed FF values. However, the ChgModB method has shown the optimum performance [25,37].

Luckily, modelling zinc-containing proteins using the bonded model has been facilitated by the development of the empirical extended zinc AMBER force field (EZAFF) method for calculating the zinc-related bond and angle parameters by Yu et al. [50]. The empirical parameters were derived from the zinc AMBER force field (ZAFF) parameters [37] which were originally calculated by the Seminario method. The empirical method is computationally economic with wider applications and has shown comparable performance to the more demanding methods with respect to relative energies calculations and accurate structural representation [50]. Moreover, the use of the bonded model has been facilitated further by its incorporation into the Metal Centre Parameter Builder (MCPB) and particularly the python-based MCPB.py tool [25,37] available in the AmberTools package [6].

However, the standard bonded model protocol produces protein-ligand complexes in which the ligand is covalently bound to the metal if any of the ligand atoms occur within the coordination distance of the metal ion. Thereby, the flexibility of the ligand is compromised during MD simulations leading to biased results. Hence, MD simulations based on the standard bonded model protocol may be improper, especially when investigating novel compounds where protein-ligand crystal structures are lacking. Thus, the bonded model representation of the ligand-metalloprotein complexes necessitates the subsequent use of sufficiently long hybrid QM/MM MD simulations to validate the binding mode.

In hybrid QM/MM MD simulations, a QM method is combined with a MM-based FF. The QM method is used to describe the interactions of a minimal part of the system, mainly the metal site and the bound ligand. Thereby, any bond-forming and/or breaking in the metal centre can be modelled. Hybrid QM/MM calculations provide a compromise between speed and accuracy and their effectiveness for studying metalloenzymes has been proved [34]. Nonetheless, these techniques are still computationally expensive. Hence, the time scales currently achievable with hybrid QM/MM MD might not allow sufficient sampling of the ligand's binding mode.

Therefore, a simple method for refining the docking solutions of ligands bound to metalloproteins using classical MD is described here. The method is based on a new modification to the standard bonded model MCPB.py method [25,37] and called the modified bonded model (MBM) approach. The approach enables a fully flexible refinement of the protein-ligand complexes despite the occurrence of ligand atoms within the metal coordination distance.

The MBM approach was validated by its ability to reproduce the native conformation of NDM-1 crystal structures. In addition, the ability of the MBM approach to predict the binding features of NDM-1 β-lactam substrates was compared to that of the intensive hybrid QM/MM calculations. The study encompassed ligands from the four β-lactam classes (penicillins, cephalosporins, carbapenems, and monobactams) to help unravel the features of β-lactam substrates recognition by NDM-1.

The binding of intact β-lactams to NDM-1 was investigated previously by protein-ligand docking [52] and also by MD [20,33,51,54]. Unlike the previous studies, the binding of intact β-lactams to NDM-1 was studied here by longer MD simulations using the new MBM approach to ensure less biased results. Therefore, this study can provide better understanding of β-lactam substrates recognition by NDM-1. Moreover, the new MBM approach can be used for MD studies of other metallo-β-lactamases and possibly other metal-containing proteins.

2. Methods

The AmberTools16 package [5] was used to prepare protein-ligand docking complexes for MD simulations. Three crystal structure complexes of NDM-1 were used; with hydrolysed ampicillin [20] (PDB code: 4HL2), with L-captopril [22] (PDB code: 4EXS), and with hydrolysed imipenem [10] (PDB code: 5YPK). The MCPB.py tool [25,37] was initially used for modelling the three complexes in four different methods; the bonded model, the non-bonded model (4n2), the non-bonded model with charge refitting (4n1), and the new modified bonded model (MBM), Fig. 1.

Ampicillin, imipenem, nitrocefin and aztreonam, Fig. 2, were docked into NDM-1 using Genetic Optimisation for Ligand Docking (GOLD) [48], from CCDC Software Ltd. The docking complexes were modelled using both the standard bonded model MCPB.py method and the MBM approach, Fig. 1. All models were solvated with a truncated octahedral water box of 8.0 Å using the tip3p water model [18]. Amber topology and coordinate files were prepared by LEaP. Afterwards, MD simulations were carried out for the crystal structure complexes, the docking complexes of intact β-lactams as well as the apo-protein using PMEMD (Particle Mesh Ewald Molecular Dynamics) [42].

MD simulations protocol involved minimization, heating, equilibration, and production. A cut-off value of 12 Å was used for nonbonded

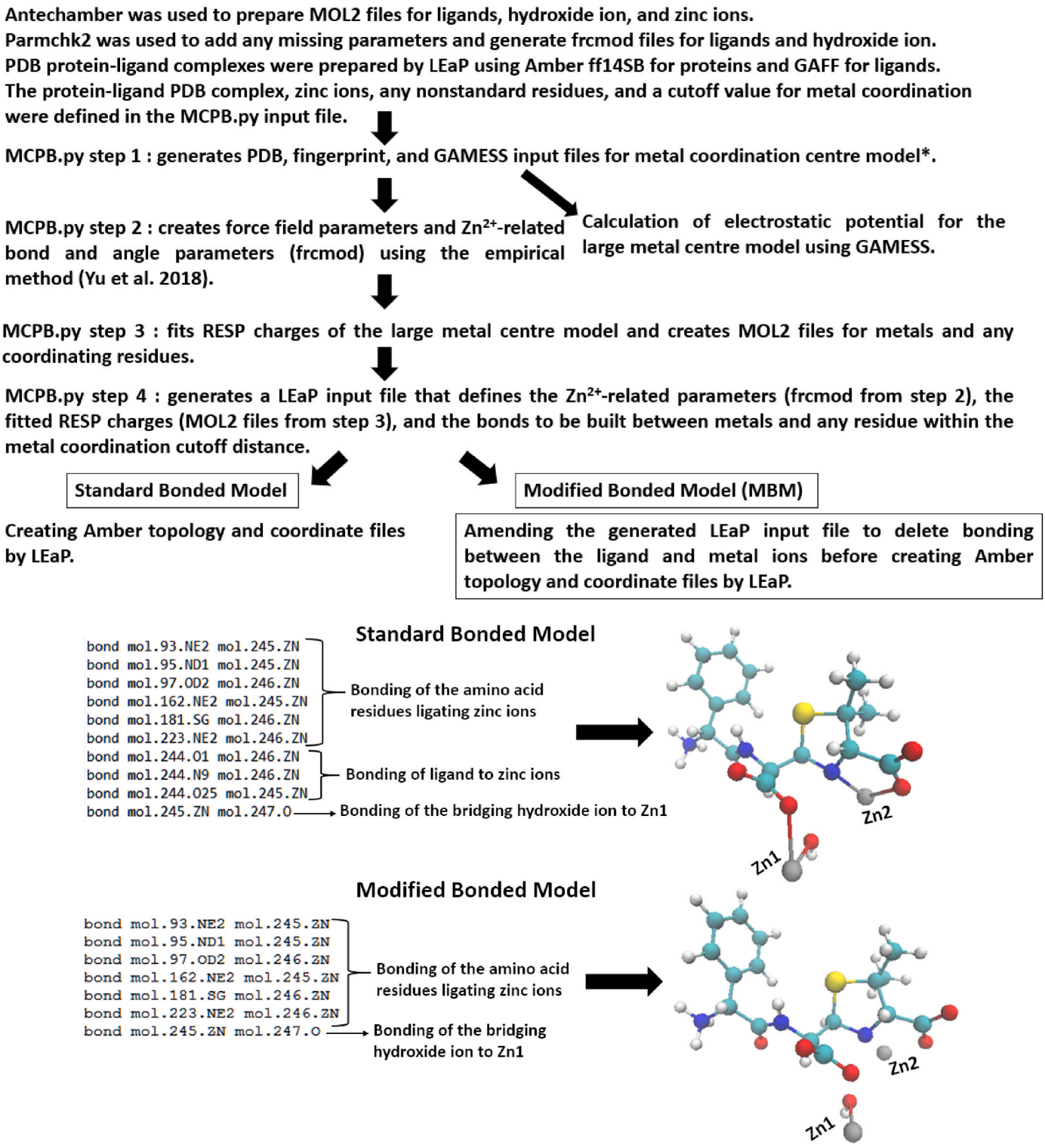

Fig. 1. Summary of the standard bonded model method and the proposed modified bonded model method. In the non-bonded model (4n2) method, MCPB.py modelling is started from step 4. In the non-bonded model with RESP charge fitting (4n1) method, step 2 is skipped. *Three models are created for the metal centre; the small model (metals, any coordinating non-amino acid residues, and any coordinating amino acid residues for which a CH_3 is used to cap the side chain), the standard model (metals, any coordinating non-amino acid residues, and any coordinating amino acid residues including their backbone atoms without capping), and the large model (metals, any coordinating non-amino acid residues, any coordinating amino acid residues for which an acetyl and/or *N*-methylamine is used to cap the backbone atoms, and the glycine residues used to link any two coordinating amino acid residues occurring within 5 Å from each other). The model showed above is for open ampicillin binding to the NDM-1 catalytic site (PDB code: 4HL2).

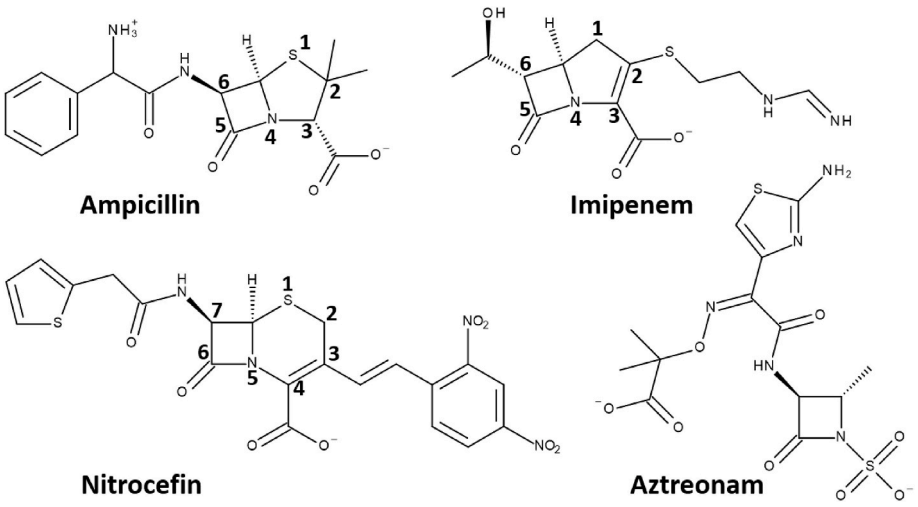

Fig. 2. Chemical structures of the β-lactams used for docking and MD simulations.

interactions. A random seed was used to start all the simulations after minimization. In minimization, the positions of all residues were restrained using a harmonic potential of 500 kcal/mol-Å^2 while the rest of the system (water and ions) was minimised at a constant volume using a combined conjugate gradient and steepest descent method. The maximum number of cycles was 2000, of which 1000 cycles were performed with the steepest descent method. The same parameters were then used to minimise the whole system without restraints.

Subsequently, the system was heated from 0 to 300 K over 20 ps using the Langevin thermostat with a collision frequency of 1 ps^{-1} [55]. Afterwards, the system was equilibrated over 5 ns at constant pressure and temperature (300 K) using the Langevin thermostat. Production was conducted at constant volume and temperature using the weak-coupling algorithm [4]. SHAKE bond length constraints were applied to constrain hydrogen atoms [40]. Wrapping was allowed and the simulation was run for 210 ns. The relaxed bonded model complexes of intact β-lactams were subsequently subjected to 100 ps hybrid QM/MM MD using the PM3 [45] and DFTB3 [12–14,32] Hamiltonians. (Further method details and chemical structures are given in the supplementary information).

3. Results and discussion

MD simulations were initially carried out for three NDM-1 crystal structures modelled using the bonded model, the non-bonded model with charge refitting (4n1), and the normal non-bonded model (4n2) [25,37].

In all the MD simulations described below, there was an initial two-stage energy minimization to relax any steric clashes and to produce an ensemble that would be stable in the MD simulations that followed. The first stage included a restraint to the positions of the protein and ligand and allowed the water and neutralising ions to be relaxed first. The second stage involved relaxation of the whole system with no restraints. For both, the restraints (or lack of them) were not relevant to, and made no difference to, any coordination bonds between the zinc ions and any other components, coordination effectively being treated as an unbreakable bond in ordinary MM MD simulations. The use of temporary restraints is a common approach either in the energy minimization phase (as presented here) or in the initial molecular dynamics stage (for example [11])

3.1. Non-bonded model

The simple non-bonded model method failed to preserve the conserved coordination geometry of the NDM-1 metal centre, Fig. S1. However, because no charge refitting was applied on the ligating residues with the 4n2 model, the relatively strong electrostatic interactions between zinc ions and the deprotonated Cys208 and Asp124 residues (Zn2 ligands) partially stabilized zinc ions in the active site, especially with the presence of the bridging hydroxide ion in the 4HL2 structure. This explains the reduced inter-metal distance compared to the 4HL2 crystal structure and the smaller RMSD of Zn2 compared to that of Zn1, Table 1.

The influence of electrostatic interactions is also manifested in the distances between each zinc ion and the coordinating atoms of its ligating residues. Only the sulfur atom of Cys208 and the OD2 oxygen of Asp124 were within coordination distance to Zn2, whereas the coordinating nitrogen of all the Zn1-histidine ligands was more than 3 Å away. By contrast, the coordination geometry of both Zn^{2+} ions was less stable when charge refitting was applied in the 4n1 model. The coordination geometry of both metals was distorted, starting from the heating stage. During equilibration, Zn1 left the active site of both the 4HL2 and the 4EXS structures, while both zinc ions left the active site of the 5YPK structure. This is reflected by the significantly increased Zn–Zn distances, Table 1.

3.2. Bonded model

In contrast, the bonded model maintained the coordination geometry of both Zn^{2+} sites throughout the simulation, which is shown by the small RMSD values of both metals as well as the reproduced experimental distances between Zn^{2+} ions, Table 1. In addition, the proteins were stable during the simulation, except for the L3 loop region. The latter was remarkably flexible compared to the L10 loop and contributed most to the protein RMSD.

In fact, the L3 loop conformation was the major variation observed by Green et al. [15] among a group of NDM-1 crystal structures. The L3 loop showed a more open conformation after 192 ns in the 4EXS simulation, while it appeared enclosing the active site after 177 ns in the 5YPK simulation, Fig. 3. The simulations of the three crystal structures revealed 3 main L3 loop conformations as described by Zhu et al. [54], Fig. 3 & S2. These backbone motions of the L3 loop may play role in binding to substrates, stabilising them during catalysis, and enhancing product release.

Because the native ligands were covalently bound to both zinc ions via their metal-ligating atoms, the binding mode of the three ligands was stable throughout the simulation, Fig. S3. However, when it comes to novel compounds or when crystal structures are lacking, the bonded model may not be appropriate for validating and refining the binding modes predicted by docking. That is because the representation of coordination interactions between any bound ligand and zinc ions by

Table 1
The average inter-zinc distances and the mean RMSD values of metals compared to the crystal structure during the 210 ns (NVT) MD simulations of the 3 crystal structures. Distances for the 4n1 model represent the 5 ns NPT MD.

Model	Zn1–Zn2 distance (Å)			Zn1 RMSD (Å)			Zn2 RMSD (Å)		
	4HL2	4EXS	5YPK	4HL2	4EXS	5YPK	4HL2	4EXS	5YPK
4n1	53	58	102	54[a]	58[a]	85[a]	2.2	0.76	47[a]
4n2	3.27	3.85	6.89	2.66	1.67	5.75	1.23	1.46	0.79
Bonded	4.58	3.53	3.91	0.45	0.37	0.38	0.37	0.37	0.51
MBM	4.34	3.38	3.75	0.64	0.45	0.44	0.51	0.50	0.53
Crystal structure	4.60	3.59	3.94						

[a] The metal left the active site.

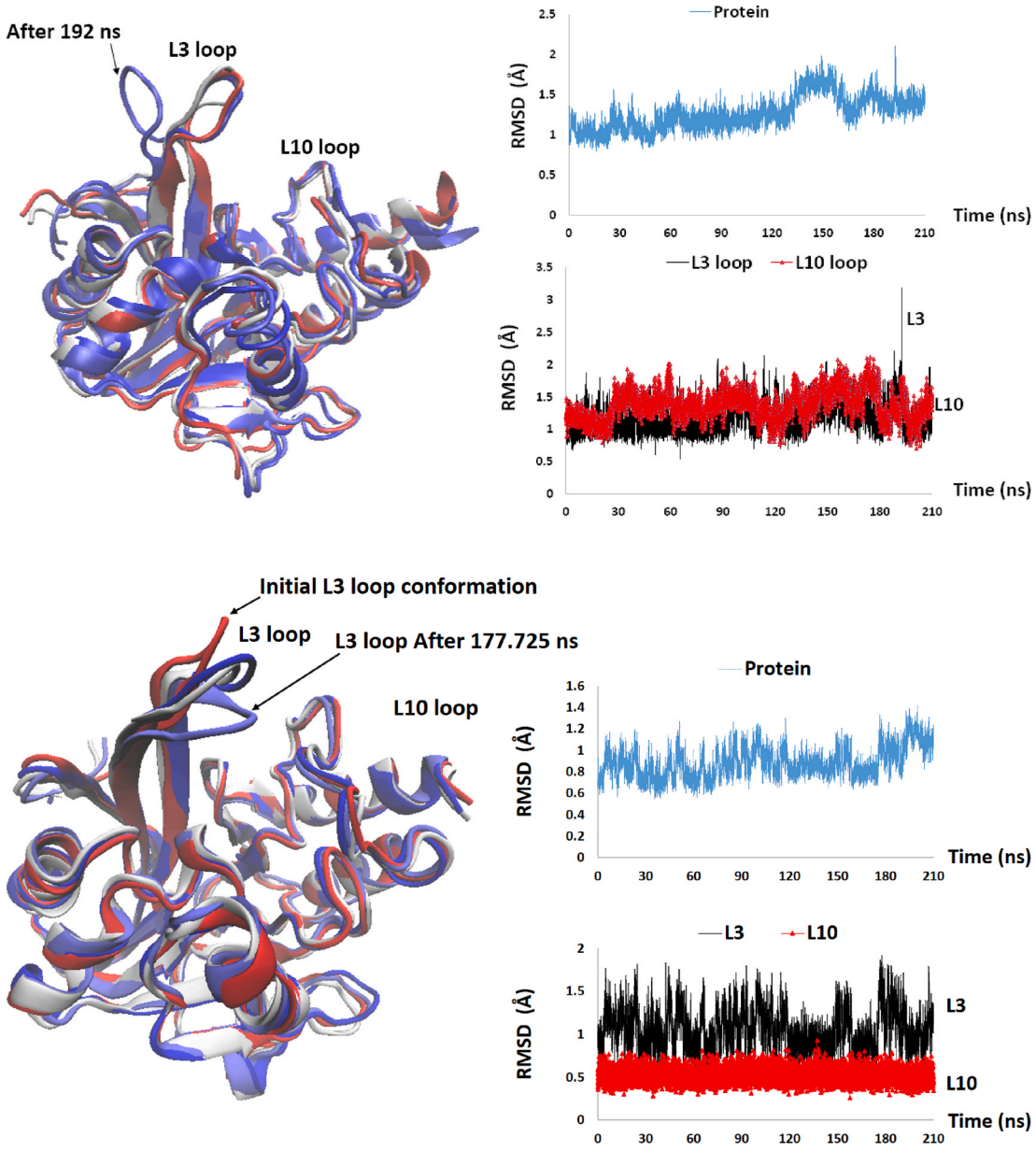

Fig. 3. The conformations of the 4EXS (top) and 5YPK (bottom) crystal structures after 105 ns (grey) and 210 ns (blue) of bonded model MD superimposed on the starting conformation (red), and the RMSD values of the protein backbone atoms relative to the crystal structure. The largest variation in the protein conformation arises from the highly flexible L3 loop mainly at 192 ns in 4EXS and at 177.725 ns in 5YPK. RMSD values were calculated for the L3 loop and the adjacent β-sheet residues (Val58-Ser75) whereas L10 represents the residues from Gly207 to Thr226. (For interpretation of the references to colour in this figure legend, the reader is referred to the Web version of this article.)

covalent bonds can hinder the flexibility of the ligand, Fig. S4. Therefore, the MBM approach was proposed.

3.3. Modified bonded model (MBM)

The leap input file generated in the last step of the MCPB.py modelling (Fig. 1, step 4) was modified by removing the bonding information between the native ligand and both zinc ions, while keeping the bonding information between zinc ions and their ligating amino acid residues. Thereby, the generated model provides a compromise between the 4n1 non-bonded model and the bonded model. Consequently, the integrity of the conserved metal sites can be maintained throughout the simulation as illustrated in Table 1. Meanwhile, the conformational space of the bound ligand can be sampled with full flexibility in the active site to gain better understanding of the ligands' binding.

Although metal coordination bonds are not explicitly described by the MBM approach, the Zn^{2+}-related force field parameters obtained by the empirical method [50], as well as the refitted RESP charges are representative of the coordination interactions with zinc ion(s). The MBM MD approach was validated by evaluating its ability to reproduce the native ligand conformation for the three NDM-1 crystal structures and predict the experimentally observed interactions with key NDM-1 residues.

Ring-opened ampicillin, which was modelled in the anionic intermediate form, was stable in the active site and a native-like binding mode was observed in ~56% of the MBM simulation. In addition, the experimentally observed interaction between the C_3-carboxylate oxygen and both the Asn220 backbone and the Lys211 side chain was observed in 20%, and 35% of simulation time, respectively. Furthermore, the average distance between the C_3-carboxylate oxygen and the Lys211 side chain nitrogen was 3.1 Å, which is comparable to the experimental distance of 2.9 Å, indicating a persistent electrostatic interaction with Lys211. However, in the last 40% of the simulation, the ligand was beyond the Zn^{2+}-coordinating distance but stabilized mainly by hydrophobic interactions with the side chains of Ile35, Met67, Phe70, Val73, His189, and His250, as well as H-bonding and electrostatic interaction between its C_3-carboxylate and the Lys211 side chain, Fig. 4.

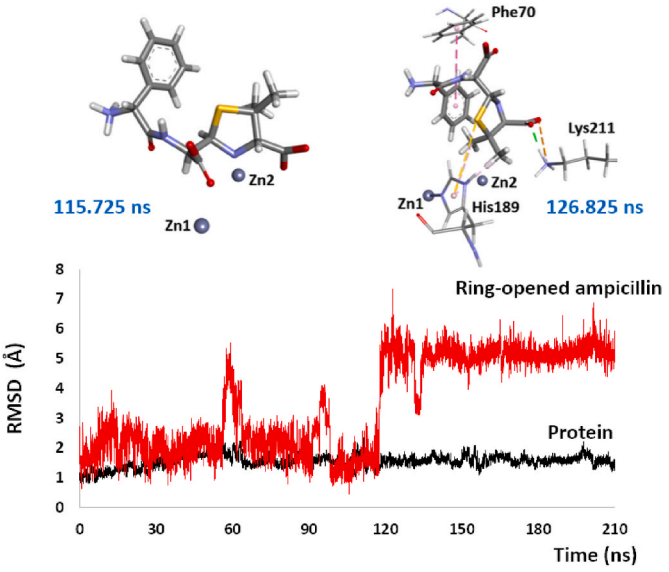

Fig. 4. The RMSD of the 4HL2 backbone atoms and the heavy atoms of its native ligand relative to the crystal structure in the MBM MD simulation. The native conformation (left) prevails before 120 ns. The main interactions of the ligand with the protein residues in the binding conformation prevailing after 120 ns (right); the carboxylate group is forming electrostatic and hydrogen bonds with the Lys211 side chain. His189 is stabilising the substrate by hydrophobic pi-alkyl and pi-sulfur bonds, and Phe70 is forming a T-shaped pi-pi stacking with the phenyl substituent, while the anionic nitrogen is exposed to solvent.

Unlike ring-opened ampicillin, ring-opened imipenem maintained a native-like binding mode throughout the MBM MD simulation, and the average ligand RMSD compared to the native conformation was 2.57 Å. The RMSD of the ligand was ≤2.5 Å in >50% of simulation time, Fig. 5. During this time, the average distances from the C_5-carboxylate oxygen to Zn1 and Zn2 were 2.8 Å and 3.5 Å, respectively, which are comparable to the experimental distances of 2.0 Å, and 3.1 Å, respectively. In addition, the average distance from the C_3-carboxylate oxygen to Zn1 and Zn2 was 5.8 Å and 4.9 Å, respectively, while the corresponding experimental distances are 5.0 Å and 3.1 Å, respectively.

Although the distances between the key ligand atoms and metal ions were not exactly reproduced, the predicted distances can describe the reactions observed experimentally. For example, it can be concluded from the simulation that the C_5-carboxylate but not the C_3-carboxylate of the ring-opened imipenem can coordinate to Zn1 (distance ≤3 Å), while the C_3-carboxylate can interact solely by electrostatic bonds with both zinc ions, which reflects the crystal structure interactions. Furthermore, the average distance between the C_3-carboxylate oxygen and the Lys211 side chain nitrogen was 2.8 Å, which is comparable to the experimental distance of 2.6 Å, indicating a persistent electrostatic interaction with Lys211. In addition, the experimentally observed H-bonding between the C_3-carboxylate oxygen and the Lys211 side chain, as well as that between the C_6-carboxylate oxygen and the Asn220 side chain were observed in ~60% and ~21% of simulation time, respectively.

The RMSD of L-captopril was within 2.5 Å from the crystal structure conformation in about 20% of the simulation, Fig. 6. L-captopril was less stable than ring-opened β-lactams in the active site, possibly due to the fewer hydrophobic contacts with the protein and the weaker interaction with the Lys211 side chain (H-bonding in 4% of simulation time compared to 35% with ring-opened ampicillin and 60% with ring-opened imipenem). The average distance between the carboxylate oxygen and the Lys211 side chain nitrogen was 6.7 Å, which is comparable to the experimental distance of 7.6 Å.

The experimentally observed H-bonding between the carboxylate oxygen of L-captopril and the Asn220 backbone was observed in ~20% of simulation time. Furthermore, the thiolate sulfur and the carbonyl oxygen were within <3 Å from at least one of the zinc ions in ~26%, and ~5% of the simulation, respectively, while the carboxylate oxygen approached Zn2 only in ~2% of the time. Thus, the inhibitory activity of L-captopril seems to originate chiefly from its non-selective thiolate interaction with the metals as observed in the crystal structure [22].

These results indicate that the MBM MD approach was able to predict the experimentally observed interactions of native ligands with NDM-1, particularly for the well-binding β-lactam hydrolysis intermediates. As an additional test, the MBM approach was further evaluated in the MD simulations of intact β-lactam substrates and compared to hybrid QM/MM MD simulations of the bonded model complexes.

3.4. Docking of intact β-lactams

In the docking complexes, ampicillin, imipenem, and nitrocefin were binding to the active site by coordination and electrostatic bonds with Zn2 via their C_3/C_4-carboxylate, whereas the coordination with Zn1 via the β-lactam oxygen was only observed with imipenem and nitrocefin. The C_3/C_4-carboxylate moiety was also H-bonded to the Asn220 backbone and forming a salt bridge with the Lys211 side chain. Although aztreonam was interacting similarly with Zn2, Asn220 and Lys211 via its sulfonate group, the β-lactam oxygen of aztreonam was coordinating to Zn2 instead of Zn1, Fig. S5. Nevertheless, the electrophilic carbon of all β-lactams was posed within <4 Å from the oxygen of the bridging water (nucleophile).

The L3 residues Met67, Phe70, and Val73, as well as Ile35, and Trp93 contributed to the β-lactams' binding by a variety of hydrophobic

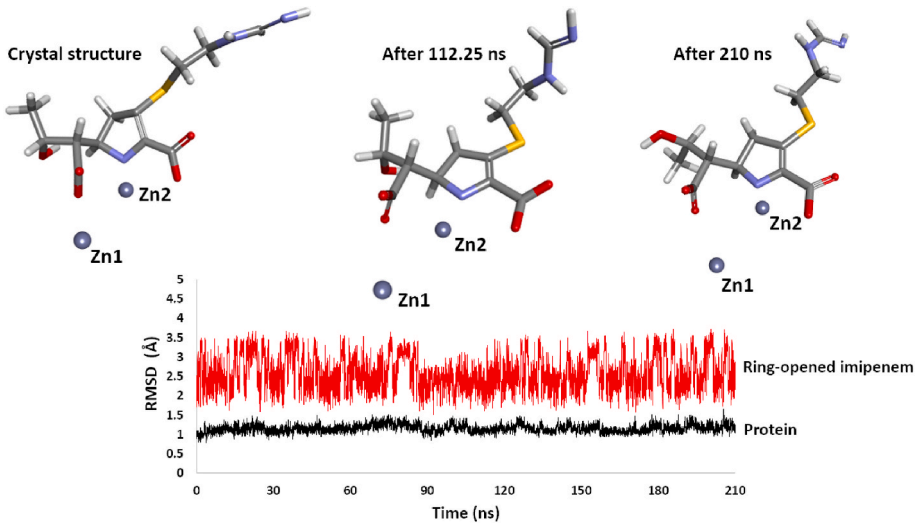

Fig. 5. The RMSD of the 5YPK backbone atoms and the heavy atoms of its native ligand relative to the crystal structure in the MBM MD simulation. A native-like binding mode is observed throughout the simulation.

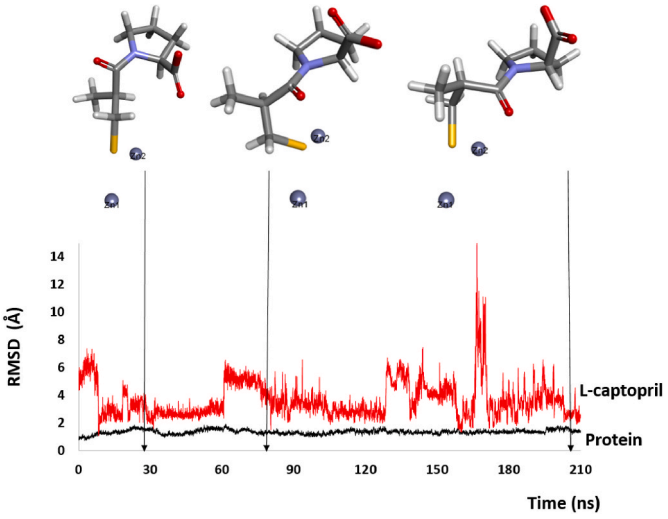

Fig. 6. The RMSD of the 4EXS backbone atoms and the heavy atoms of its native ligand relative to the crystal structure in the MBM MD simulation. A native-like binding mode is observed in the various simulation stages. The displayed binding modes represent snapshots taken after 31.6 ns, 80.45 ns, and 208.825 ns.

interactions. His250 was the only Zn^{2+}-ligating residue forming hydrophobic bonds with the ring fused to the β-lactam ring of the substrates and the methyl substituent of the aztreonam ring, Fig. S5. It is worth mentioning that the inhibitory binding mode of aztreonam reported by Yuan et al. [52]; in which the sulfonate group of aztreonam displaces the bridging nucleophile, was not observed in this docking study, while the poses of the bicyclic β-lactams resembled the substrate conformation predicted previously using AutoDock [52].

3.5. MBM MD simulations of β-lactams

During the MBM simulations, the bicyclic β-lactams ampicillin, nitrocefin, and imipenem were remarkably more stable in the active site compared to the monobactam aztreonam, Fig. 7 & S6, Table S1, which is consistent with the known NDM-1 preference for bicyclic β-lactams. Furthermore, the penicillin was less stable compared to the cephalosporin and the carbapenem substrates, which is also consistent with the experimentally observed higher binding affinity of the latter two compared to the former. For example, in the Thomas et al. [46] study, the experimental Michaelis constant values (K_m) for nitrocefin, imipenem, and ampicillin were 1.3 ± 0.2 μM, 45 ± 2 μM, and 310 ± 30 μM, respectively. However, all the β-lactam-bound proteins showed significantly more stable L3 and L10 loop regions compared to the apo-protein as shown by the average loop RMSD values in Table S1, and the loop RMSF values in Fig. 7 & S6. Stabilization of the loops refers to the formation of multiple favorable hydrophobic and polar interactions with the L3 and L10 loop residues, respectively, by the four β-lactams.

In the MBM MD simulations, at least one carboxylate oxygen was within the coordination distance (≤3 Å) of Zn2 in ~30%, ~60%, and ~5% of the simulation for ampicillin, nitrocefin, and imipenem, respectively. In a repeat set of simulations, the percentages were ~65%, ~70%, and ~9%, for ampicillin, nitrocefin, and imipenem, respectively. In aztreonam, at least one sulfonate oxygen was within the coordination distance of Zn2 in ~15%, and ~43% of the first and the second simulation, respectively. Furthermore, the C_3/C_4-carboxylate of the substrates as well as the aztreonam sulfonate were within 5 Å from Zn2 in >70% of all the trajectories. By contrast, in >70% of all simulations, the β-lactam oxygen and the β-lactam nitrogen of all the β-lactams were >3 Å away from Zn1, and Zn2, respectively, Table S2.

These findings indicate that the coordination interaction between the β-lactam oxygen and Zn1 as well as between the β-lactam nitrogen and Zn2 is unlikely in the Michaelis complex and expected to commence later during catalysis, which agrees with previous hybrid QM/MM MD findings [47,53]. However, β-lactams are expected to interact electrostatically via the C_3/C_4-carboxylate with Zn2 in the Michaelis complex. In addition, the carboxylate oxygen was within 5 Å of Zn1 in the majority of bicyclic substrates' trajectories, indicating the possibility of electrostatic interactions between the carboxylate and Zn1 in the Michaelis complexes of these substrates.

Although earlier computational studies suggested the absence of the Zn2–C_3/C_4-carboxylate coordination interaction in the NDM-1 Michaelis complexes of ampicillin and meropenem [47,53], our results indicate that the latter interaction is likely but might be dependent on the substrate structure. For example, the simulations indicate that the latter interaction is more likely with ampicillin and nitrocefin than with imipenem. Monitoring the Zn2 site coordination by rapid-freeze-quench mixing and X-ray absorption spectroscopy revealed the formation of a coordination bond between the C_3-carboxylate and Zn2 in the Michaelis complex of imipenem with monozinc B2 and B3 metallo-β-lactamases [29]. However, the Michaelis complex of imipenem with the dizinc B1 metallo-β-lactamases (NDM-1) can be different.

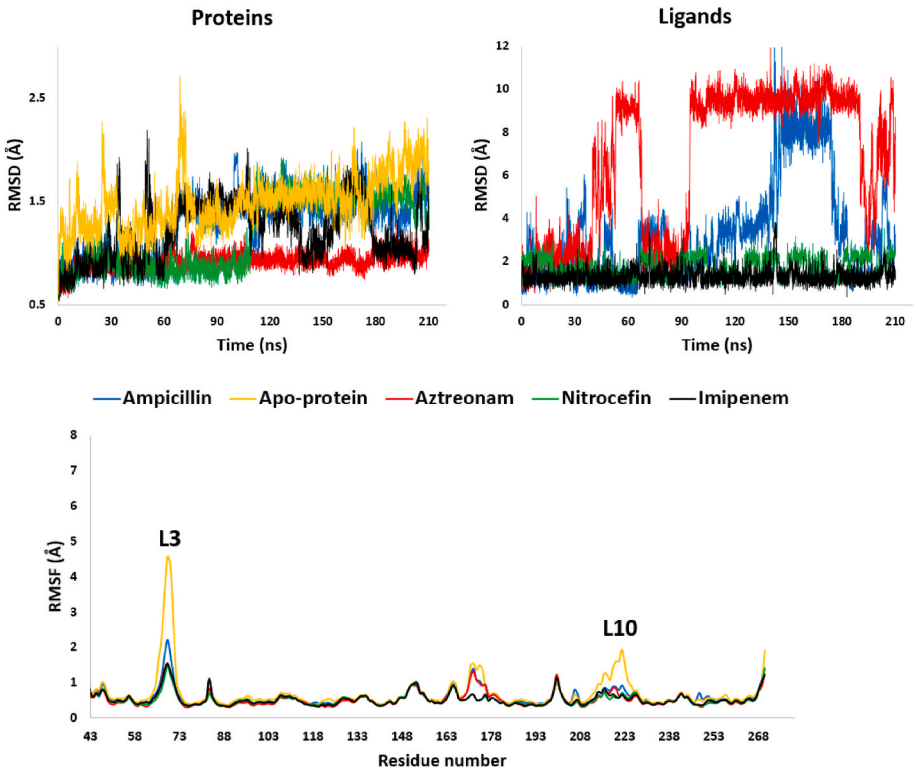

Fig. 7. The RMSD values of the protein backbone atoms and the heavy atoms of the docked β-lactams and the RMSF values of all protein residues in the β-lactam-NDM-1 complexes and the unbound protein during the MBM MD simulations.

The β-Lactam substrates are probably recognized by their carboxylate group interaction with the Lys211 side chain. Although H-bonding with the latter was not significantly frequent, the Lys211 side chain was within the range of electrostatic interactions in the majority of the imipenem and nitrocefin simulations, Table 2. However, the latter interaction was observed in <50% of both ampicillin simulations, while with aztreonam, this interaction was observed in >70% of the second simulation only. The anticipated Lys211 role is in agreement with previous computational studies [49,53,54] as well as the substantially reduced hydrolytic activity of the Lys211Glu and Lys211Ala NDM-1 mutants [27]. Nonetheless, the latter study was limited to meropenem and the abolished activity might be related to a catalytic role rather than a binding role of Lys211.

Table 2
The frequency of H-bonding between the key functional groups of the four β-lactams and both Asn220 and Lys211 as well as the average distances to the Lys211 side chain. A distance cutoff of 3 Å and an angle cutoff of 160° were used to define H-bonds. Distances are reported for the carboxylate/sulfonate oxygen atom showing the smallest average distance to the Lys211 side chain N.

Ligand	Asn220 backbone (N) with C_3/C_4–COO^-	Asn220 side chain with β-lactam O	Lys211 side chain with C_3/C_4–COO^-	Lys211(N)–C_3/C_4–COO^- distance
Nitrocefin 1st	19.5%	<1%	4%	4.2 Å
Nitrocefin 2nd	27%	<1%	8%	3.1 Å
Imipenem 1st	13%	9%	<1%	5.0 Å
Imipenem 2nd	7%	5.5%	5%	3.9 Å
Ampicillin 1st	12.5%	10%	<1%	7.6 Å
Ampicillin 2nd	31.5%	20%	<1%	5.3 Å
Aztreonam 1st	<1%[a]	<1%	<1%[a]	7.8 Å[a]
Aztreonam 2nd	8.5%[a]	0%	6%[a]	4.5 Å[a]

[a] In aztreonam, interactions with Lys211 and the Asn220 backbone were estimated for the sulfonate moiety.

Despite the assumed role of Asn220 in catalysis [22,53], it seems to be less influential than Lys211 during the initial substrate binding, Table 2. For example, H-bonding between the Asn220 backbone and the substrate C_3/C_4-carboxylate was observed in ≤30% of all the simulations. Furthermore, the Asn220 side chain showed H-bonding with the β-lactam carbonyl oxygen in ≤20% of all the simulations. Although the latter interaction is observed in the crystal structures of ring-opened substrates, it seems to be more prevalent during catalysis than in the Michaelis complex.

Nevertheless, the role of Lys211 and Asn220 in substrate binding may vary based on the structure of the substrate. The Duan et al. [8] MD study revealed five probable pathways for meropenem to enter the active site. Therefore, the mechanism of substrate recognition may depend on the gate through which the substrate enters the active site, which in turn could be controlled by the size and the nature of the substituents attached to the C_2/C_3 and C_6/C_7 position, Fig. 2. For example, the ampicillin carboxylate electrostatic interaction with the Lys211 side chain was less significant compared to that observed with nitrocefin and imipenem. Meanwhile, H-bonding between the carbonyl oxygen and the Asn220 side chain was observed only with ampicillin and imipenem. These observations imply that both residues can participate in guiding the substrate to the catalytic centre based on the substrate and its entrance pathway. These mutual roles can also explain the broad substrate specificity of NDM-1.

Although metal coordination bonds are not explicitly described by the MBM approach, the substrates maintained their interactions with NDM-1 during the simulations. This indicates that the NDM-1 binding cavity, apart from the metal ions, can strongly bind to β-lactam substrates by several residues forming hydrophobic interactions such as

Trp93, Phe70, Met67, Val73, His250 and Ile35, as well as polar interactions like those offered by Lys211, Asn220, Lys216, Ser217, and Gln123, Fig. S7.These observations are consistent with the Wang & Cheng [49] findings.

In contrast to our findings, the MD study conducted by Zhu et al. [54] revealed the prevalence of H-bonding between the Asn220 side chain and the carbonyl oxygen during the majority of the 30 ns simulations of ampicillin, nitrocefin, and meropenem. Other conflicting results were reported by Kim et al. [20] based on their 10ns MD using CHARMM. The authors referred to the persistence of coordination bonds between the β-lactam substrates and both Zn1 and Zn2 via the carbonyl oxygen and the C_3/C_4-carboxylate oxygen, respectively. Moreover, Kim et al. [20] excluded the contribution of any polar residues in substrate binding and confined this role to the metal ions and the lipophilic loop residues. However, these observations originated from very short simulations.

Although crystal structures for NDM-1 and intact β-lactams are lacking, a cyclobutanone penem analogue has been recently co-crystallised with the B1 MBL "SPM-1" (PDB code: 5NDB), which is regarded the closest available experimental model to the MBL-β-lactam Michaelis complex, Fig. S8. In this crystal structure, the bicyclic β-lactam-like core was interacting via its carboxylate substituent with Zn2 and the side chain of the neighboring lysine residue, which is the counterpart of the NDM-1 Lys211 residue. No coordination bond between the carbonyl oxygen and Zn1 exists in the crystal structure though the carboxylate oxygen is close enough to bind to Zn1 electrostatically. Other interactions included hydrophobic bonds with the loop residues flanking the active site, and the Zn2-ligating histidine [1]. These experimental observations support the Michaelis complex features predicted by our MBM MD, and refute theKim et al. [20] assumptions.

3.6. Binding of aztreonam to NDM-1

Although no NDM-1 conformational changes were detected by NMR upon adding 2.5 mM aztreonam [41] Lohans et al. [31] illustrated, by NMR and UV–visible spectroscopy, the NDM-1 ability to bind to aztreonam and hydrolyse it slowly with a K_m of ~9 mM, and a K_{cat} of ~0.01 s^{-1}. However, the binding mode of aztreonam to NDM-1 is still unknown. Based on our MBM MD results, aztreonam seems to have the ability to bind to Zn2 via the sulfonate oxygen(s), and stabilise the L3 region by hydrophobic interactions resembling the real substrates, Fig. S7. These results coincide with the NMR spectral changes detected by Poeylaut-palena et al. [38] upon adding aztreonam to the B1 MBL BcII.

Although the β-lactam carbonyl carbon of aztreonam was orientated away from the bridging nucleophile for the majority of both simulations, it was accessible to the nucleophile (within 3.2–4.0 Å) in a few frames in the second simulation. By contrast, the carbonyl carbon of the bicyclic β-lactams was predominantly within 3 Å from the nucleophilic hydroxide oxygen in all simulations, Fig. 8 & S9.

Nonetheless, the Asn220 side chain was not interacting with the aztreonam β-lactam oxygen. In addition, the average distance between the β-lactam oxygen and Zn1 was >7 Å in both simulations, while the latter distance was between 3 and 5 Å in the simulations of the bicyclic substrates. These observations might explain the relative stability of aztreonam against NDM-1 since both Zn1 and the Asn220 side chain are supposed to facilitate the nucleophile addition by polarising the β-lactam carbonyl group, and stabilising the hydrolysis intermediate by forming an oxyanion hole [22]. These findings indicate the importance of the bicyclic core for effective substrate binding.

In both simulations, aztreonam was binding to NDM-1 crystal structures whose native ligands are bicyclic substrates. Therefore, to validate the suggested binding mode of aztreonam, a third simulation was run with aztreonam binding to the apo-protein structure, PDB code: 3SPU [21], Fig. S10. During the third simulation, the average distance between the β-lactam oxygen and Zn1 was 10 Å, while at least one sulfonate oxygen was within 3–5 Å from Zn2 in ~10–15% of the trajectory. In addition, the sulfonate oxygen(s) formed electrostatic and hydrogen bonds with the Lys211 side chain in 73%, and 22% of the simulation, respectively. Again, no interaction was observed between the β-lactam oxygen and the Asn220 side chain, and the β-lactam carbonyl carbon was predominantly >5 Å away from the nucleophile, Fig. S11. Overall, the three simulations indicate that aztreonam binds non-productively to NDM-1, possibly to Zn2 and Lys211 via its sulfonate group while positioning the β-lactam oxygen away from Zn1 and the Asn220 side chain.

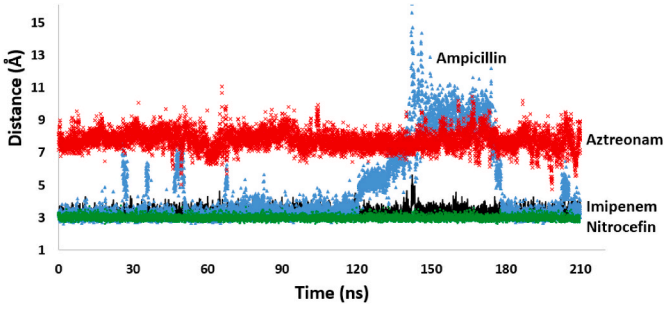

Fig. 8. The distance between the electrophilic carbonyl carbon of the β-lactam ring and the oxygen atom of the bridging nucleophilic hydroxide in the MBM MD simulations of the β-lactam-NDM-1 complexes.

3.7. Hybrid QMMM MD simulations of bonded models

During the hybrid QM/MM MD simulations of the bonded models, both QM methods broke the β-lactam coordination bonds with both zinc ions except that between Zn2 and the carboxylate oxygen of both ampicillin and imipenem, Table 3. Another exception is the AMBER/DFTB3 simulation of nitrocefin in which the bridging hydroxide was added to the carbonyl carbon while cleaving the amide bond resulting in an anionic intermediate coordinating to Zn2 via its nitrogen.

Overall, our hybrid simulations refer to the lack of coordination bonds between the carbonyl oxygen of β-lactams and Zn1 as well as between the β-lactam nitrogen and Zn2 in the Michaelis complex, Table 3, which agrees with the MBM MD predictions discussed above and previous hybrid QM/MM studies [47,53]. In addition, the only coordination interaction expected to exist in the Michaelis complex is that between the C_3/C_4-carboxylate and Zn2, which can also be dependent on the β-lactam structure. However, the hybrid QM/MM MD simulations carried out in this work were too short to provide a clear insight into the β-lactam interactions with the NDM-1 active site residues before catalysis. Longer simulations would be very computationally expensive as

Table 3
The distances between the key atoms of β-lactams and zinc ions after QMMM MD equilibration of the relaxed bonded model complexes for 100 ps. The distances at 0 ps represent the distances observed after 210 ns bonded model MD.

Ligand	β-lactam O–Zn1 (Å)		C_3/C_4–COO^--Zn2 (Å)		β-lactam N–Zn2 (Å)	
	0 ps	100 ps	0 ps	100 ps	0 ps	100 ps
Nitrocefin PM3	2.1	5.0	2.0	6.2	2.7	5.7
Nitrocefin DFTB3[a]	2.1	2.6[a]	2.0	2.4[a]	2.7	2.0[a]
Imipenem PM3	2.2	5.3	2.0	2.1	2.4	4.5
Imipenem DFTB3	2.2	4.8	2.0	6.0	2.4	5.6
Ampicillin PM3	3.4	6.3	1.9	2.2	2.9	5.1
Ampicillin DFTB3	3.4	3.8	1.9	2.1	2.9	3.2
Aztreonam PM3	2.2[b]	6.3[b]	2.3[c]	7.5[c]	3.1	8.2
Aztreonam DFTB3	2.2[b]	5.5[b]	2.3[c]	3.8[c]	3.1	6.4

[a] Nitrocefin was ring-opened in this simulation and the β-lactam N was coordinating to Zn2.
[b] The distance of aztreonam β-lactam O was measured to Zn2.
[c] The distance to Zn2 was measured for the sulfonate oxygen closest to Zn2.

only 0.02–0.04 ns could be achieved per day, depending on the number of QM atoms and processors used.

On the other hand, hundreds of nanoseconds are achievable per day with classical MD, allowing for adequate sampling. Furthermore, the results indicate that the MBM MD approach was able to describe the main features of NDM-1 motions and substrate specificity reasonably. Moreover, the MBM MD predictions were consistent with the results obtained from the short intensive hybrid QM/MM MD simulations. Thus, the MBM MD seems promising for the computational studies of NDM-1 and might be more fruitful than the bonded model MD.

3.8. Potential MBM MD applications

The MBM MD approach can be used to study the interactions of NDM-1 substrates and/or inhibitors. Although the approach may not be able to describe coordination interactions with zinc ions, the method can provide insight into the other binding interactions and the accessibility of any ligand to the metal centre. The approach would be particularly useful in studying substrate-like mechanism-based inhibitors of NDM-1 or other metallo-β-lactamases. By running MBM MD, the ability of the designed inhibitors to bind to NDM-1 productively can be investigated without the bias caused by the covalent bonds of the bonded model. In addition, the accessibility of the ligand to the metal centre and the nucleophile can be evaluated more reliably by running long MBM MD simulations.

However, given the intrinsic limitations of classical force fields, MBM MD cannot eliminate the need for hybrid QM/MM MD. The latter are still essential to simulate chemical reactivity in the active site. Nonetheless, in the absence of structural data, starting hybrid QM/MM calculations and enhanced sampling of catalytic reactions from a bonded model built from a docking complex or a crystal structure conformation of a hydrolysed substrate might be misleading. Therefore, MBM MD can be used initially to validate and refine the docking pose and choose a more reasonable starting structure for hybrid QM/MM MD simulations.

Several metalloproteins are interesting targets in drug discovery [17,23,30,39,43]. In addition, the MCPB.py tool allows the use of numerous AMBER FFs for more than 80 metals. Furthermore, parametrisation can be accomplished by either the Seminario method [44], or the Z-matrix method, in addition to the fast empirical method available for zinc [50]. Moreover, the built AMBER topology and coordinate files can be transformed into the formats utilised by other common FFs [25]. Therefore, the suggested MCPB.py-based MBM approach can have broader applications.

4. Conclusion

MD simulations of metalloproteins have been facilitated by the development of the MCPB.py program [25,37], which offers three different modelling approaches. However, only the bonded model approach reproduced the conserved coordination geometry of both NDM-1 zinc sites. Nonetheless, the bonded model approach tends to restrict the flexibility of the bound ligand in the presence of coordination bonds with zinc ions since they are treated as covalent bonds. Thus, when crystal structures are lacking, as with unhydrolysed β-lactams, the exploration of the conformations of the coordinated ligands via the bonded model MD might be futile since the models will be significantly biased by the starting structures. Therefore, the MBM approach was proposed. The MBM MD approach was validated by its ability to reproduce three crystal structure conformations of NDM-1.

The MBM approach was also applied in the MD of NDM-1 substrates from the four β-lactam classes. The results indicate that nitrocefin and imipenem bind more tightly to NDM-1 than ampicillin, which is consistent with the experimental kinetic studies. In addition, these three real substrates maintained a productive binding mode in which the β-lactam carbonyl is accessible to the nucleophile and Zn1. By contrast, this study suggested a less productive binding mode for the poorly-hydrolysable aztreonam, which is concordant with the previously reported NMR studies as well as the aztreonam relative stability against NDM-1. These findings imply that the MBM approach described the β-lactam binding interactions reasonably.

In contrast to a previous MD study [20], the results imply that the substrates may be directed to the catalytic center by the cooperation of the polar L10 loop residues such as Lys211, Asn220 and hydrophobic residues including Trp93, Ile35, and the L3 loop residues. In addition, bicyclic β-lactam substrates are predicted to coordinate to Zn2 but not to Zn1 in the Michaelis complex, which contradicts the docking predictions as well as the crystal structures of hydrolysed substrates. Furthermore, the anticipated features of the bicyclic β-lactam-NDM-1 Michaelis complexes are in agreement with the crystal structure of the B1 MBL "SPM-1" complexed with a cyclobutanone penem analogue, which resembles the bicyclic β-lactam substrates [1].

Moreover, the MBM MD results agreed with the hybrid QM/MM MD simulations. Therefore, the MBM approach seems promising for studying ligands' binding with NDM-1 and other MBLs and can particularly help in the design and discovery of mechanism-based MBL inhibitors. The MBM MD approach allows for sufficient sampling which might not be feasible with the currently achievable time scales with hybrid QM/MM MD. The MBM approach can be used to validate and refine the docking pose when crystal structures are lacking. It can also help in the identification of a reasonable starting structure for subsequent hybrid QM/MM MD simulations and enhanced sampling of catalytic reactions. Considering the versatile force fields and parametrisation methods offered by the MCPB.py tool for numerous metals, the proposed MBM approach will be useful in the investigation of other metalloproteins of interest.

Declaration of competing interest

The authors declare that they have no known competing financial interests or personal relationships that could have appeared to influence the work reported in this paper.

Data availability

Data will be made available on request.

Appendix A. Supplementary data

Supplementary data to this article can be found online at https://doi.org/10.1016/j.jmgm.2023.108431.

References

[1] M.I. Abboud, M. Kosmopoulou, A.P. Krismanich, J.W. Johnson, P. Hinchliffe, J. Brem, T.D.W. Claridge, J. Spencer, C.J. Schofield, G.I. Dmitrienko, Cyclobutanone mimics of intermediates in metallo-β-lactamase catalysis, Chemistry 24 (2018) 5734–5737.
[2] J. Aqvist, A. Warshel, Free energy relationships in metalloenzyme-catalyzed reactions. Calculations of the effects of metal ion substitutions in staphylococcal nuclease, J. Am. Chem. Soc. 112 (8) (1990) 2860–2868.
[3] C.I. Bayly, P. Cieplak, W.D. Cornell, P.A. Kollman, A well-behaved electrostatic potential based method using charge restraints for deriving atomic charges: the RESP model, J. Phys. Chem. 97 (40) (1993) 10269–10280.
[4] H.J.C. Berendsen, J.P.M. Postma, W.F. van Gunsteren, A. DiNola, J.R. Haak, Molecular dynamics with coupling to an external bath, J. Chem. Phys. 81 (8) (1984) 3684–3690.
[5] D.A. Case, R.M. Betz, W. Botello-Smith, D.S. Cerutti, T.E.I. Cheatham, T.A. Darden, R.E. Duke, T.J. Giese, H. Gohlke, A.W. Goetz, N. Homeyer, S. Izadi, P. Janowski, J. Kaus, A. Kovalenko, T.S. Lee, S. LeGrand, P. Li, C. Lin, T. Luchko, R. Luo, B. Madej, D. Mermelstein, K.M. Merz, G. Monard, H. Nguyen, H.T. Nguyen, I. Omelyan, A. Onufriev, D.R. Roe, A. Roitberg, C. Sagui, C.L. Simmerling, J. Swails, R.C. Walker, J. Wang, R.M. Wolf, X. Wu, L. Xiao, D.M. York, P. A. Kollman, AMBER 2016, 2016.
[6] D.A. Case, H.M. Aktulga, K. Belfon, I.Y. Ben-Shalom, J.T. Berryman, P.A. Kollman, et al., Amber 2022, 2022.
[7] M. de Vivo, M. Masetti, G. Bottegoni, A. Cavalli, Role of molecular dynamics and related methods in drug discovery, J. Med. Chem. 59 (9) (2016) 4035–4061.

[8] J. Duan, C. Hu, J. Guo, L. Guo, J. Sun, Z. Zhao, A molecular dynamics study of the complete binding process of meropenem to New Delhi metallo-β-lactamase 1, Phys. Chem. Chem. Phys. 20 (2018) 6409–6420.
[9] J.D. Durrant, J.A. Mccammon, Molecular dynamics simulations and drug discovery, BMC Biol. 9 (71) (2011) 1–9.
[10] H. Feng, X. Liu, S. Wang, J. Fleming, D. Wang, W. Liu, The mechanism of NDM-1-catalyzed carbapenem hydrolysis is distinct from that of penicillin or cephalosporin hydrolysis, Nat. Commun. 8 (2017), 2242–2242.
[11] Y.H. Fung, W.P. Kong, A.S.L. Leung, R. Du, P.K. So, W.L. Wong, Y.C. Leung, Y. W. Chen, K.Y. Wong, NDM-1 Zn1-binding residue His116 plays critical roles in antibiotic hydrolysis, Biochim. Biophys. Acta, Proteins Proteomics 1870 (10) (2022), 140833.
[12] M. Gaus, Q. Cui, M. Elstner, DFTB3 : extension of the self-consistent-charge density-functional tight-binding method (SCC-DFTB), J. Chem. Theor. Comput. 7 (2011) 931–948.
[13] M. Gaus, A. Goez, M. Elstner, Parametrization and benchmark of DFTB3 for organic molecules, J. Chem. Theor. Comput. 9 (2013) 338–354.
[14] M. Gaus, X. Lu, M. Elstner, Q. Cui, Parameterization of DFTB3/3OB for sulfur and phosphorus for chemical and biological applications, J. Chem. Theor. Comput. 10 (2014) 1518–1537.
[15] V.L. Green, A. Verma, R.J. Owens, S.E.V. Phillips, S.B. Carr, Structure of New Delhi metallo-β-lactamase 1 (NDM-1), Acta Crystallogr. F67 (2011) 1160–1164.
[16] P.W. Groundwater, S. Xu, F. Lai, L. Váradi, J. Tan, J.D. Perry, D.E. Hibbs, New Delhi metall-β-lactamase-1: structure, inhibitors and detection of producers, Future Med. Chem. 8 (9) (2016) 993–1012.
[17] L. Guasch, A.V. Zakharov, O.A. Tarasova, V.V. Poroikov, C. Liao, M.C. Nicklaus, Novel HIV-1 integrase inhibitor development by virtual screening based on QSAR models, Curr. Top. Med. Chem. 16 (4) (2016) 441–448.
[18] W.L. Jorgensen, J. Chandrasekhar, J.D. Madura, R.W. Impey, M.L. Klein, Comparison of simple potential functions for simulating liquid water, J. Chem. Phys. 79 (2) (1983) 926–935.
[19] L. Ju, Z. Cheng, W. Fast, R.A. Bonomo, M.W. Crowder, The continuing challenge of metallo- β -lactamase inhibition : mechanism matters, Trends Pharmacol. Sci. (2018) 1–13.
[20] Y. Kim, M.A. Cunningham, J. Mire, C. Tesar, J. Sacchettini, A. Joachimiak, NDM-1, the ultimate promiscuous enzyme: substrate recognition and catalytic mechanism, Faseb. J. 27 (5) (2013) 1917–1927.
[21] D. King, N. Strynadka, Crystal structure of New Delhi metallo-β-lactamase reveals molecular basis for antibiotic resistance, Protein Sci. 20 (2011) 1484–1491.
[22] D.T. King, L.J. Worrall, R. Gruninger, N.C.J. Strynadka, New Delhi metallo-beta-lactamase: structural insights into beta-lactam recognition and inhibition, J. Am. Chem. Soc. 134 (2012) 11362–11365.
[23] J. Kollar, V. Frecer, Diarylcyclopropane hydroxamic acid inhibitors of histone deacetylase 4 designed by combinatorial approach and QM/MM calculations, J. Mol. Graph. Model. 85 (2018) 97–110.
[24] P. Li, K.M. Merz, Taking into account the ion-induced dipole interaction in the nonbonded model of ions, J. Chem. Theor. Comput. 10 (2014) 289–297.
[25] P. Li, K.M.J. Merz, MCPB.py: a Python based metal center parameter builder, J. Chem. Inf. Model. 56 (4) (2016) 599–604.
[26] P. Li, B.P. Roberts, D.K. Chakravorty, K.M. Merz, Rational design of particle Mesh Ewald compatible Lennard-Jones parameters for +2 metal cations in explicit solvent, J. Chem. Theor. Comput. 9 (2013) 2733–2748.
[27] Z. Liang, L. Li, Y. Wang, L. Chen, X. Kong, Y. Hong, L. Lan, M. Zheng, C. Guang-Yang, H. Liu, X. Shen, C. Luo, K.K. Li, K. Chen, H. Jiang, Molecular basis of NDM-1, a new antibiotic resistance determinant, PLoS One 6 (8) (2011) 1–8.
[28] F. Lin, R. Wang, Systematic derivation of AMBER force field parameters applicable to zinc-containing systems, J. Chem. Theor. Comput. 6 (6) (2010) 1852–1870.
[29] M. Lisa, A.R. Palacios, M. Aitha, M.M. González, D.M. Moreno, M.W. Crowder, R. A. Bonomo, J. Spencer, D.L. Tierney, L.I. Llarrull, A.J. Vila, A general reaction mechanism for carbapenem hydrolysis by mononuclear and binuclear metallo-β-lactamases, Nat. Commun. 8 (538) (2017) 1–11.
[30] S. Liu, L. Jing, Z. Yu, C. Wu, Y. Zheng, E. Zhang, Q. Chen, Y. Yu, L. Guo, Y. Wu, G.-B. Li, ((S)-3-Mercapto-2-methylpropanamido)acetic acid derivatives as metallo-β -lactamase inhibitors : synthesis , kinetic and crystallographic studies, Eur. J. Med. Chem. 145 (2018) 649–660.
[31] C.T. Lohans, J. Brem, C.J. Schofield, New Delhi Metallo-β-lactamase 1 catalyzes avibactam and aztreonam hydrolysis, Antimicrob. Agents Chemother. 61 (12) (2017) 1–3.
[32] X. Lu, M. Gaus, M. Elstner, Q. Cui, Parametrization of DFTB3/3OB for magnesium and zinc for chemical and biological applications, J. Phys. Chem. B 119 (2015) 1062–1082.
[33] F. Marcoccia, H.S. Leiros, M. Aschi, G. Amicosante, M. Perilli, Exploring the role of L209 residue in the active site of NDM-1 a metallo- β -lactamase, PLoS One 13 (1) (2018) 1–12.
[34] A.J. Mulholland, Chemical accuracy in QM/MM calculations on enzyme-catalysed reactions, Chem. Cent. J. 1 (19) (2007) 1–5, link.springer.com/article/10.1186/1752-153X-1-19/fulltext.html.
[35] M.R. Nechay, C.E. Valdez, A.N. Alexandrova, Computational treatment of metalloproteins, J. Phys. Chem. B 119 (2015) 5945–5956.
[36] Y. Pang, K.U.N. Xu, J.E.L. Yazal, F.G. Prendergast, Successful molecular dynamics simulation of the zinc-bound farnesyltransferase using the cationic dummy atom approach, Protein Sci. 9 (10) (2000) 1857–1865.
[37] M.B. Peters, Y. Yang, B. Wang, L. Füsti-Molnár, M.N. Weaver, K.M.J. Merz, Structural survey of zinc-containing proteins and development of the Zinc AMBER Force Field (ZAFF), J. Chem. Theor. Comput. 6 (9) (2010) 2935–2947.
[38] A.A. Poeylaut-palena, P.E. Tomatis, A.I. Karsisiotis, C. Damblon, E.G. Mata, A. J. Vila, A minimalistic approach to identify substrate binding features in B1 Metallo-β -lactamases, Bioorg. Med. Chem. Lett 17 (2007) 5171–5174.
[39] A. Proschak, J. Kramer, E. Proschak, T.A. Wichelhaus, Bacterial zincophore [S , S] -ethylenediamine-N , N'-disuccinic acid is an effective inhibitor of MBLs, J. Antimicrob. Chemother. 73 (2018) 425–430.
[40] J.-P. Ryckaert, G. Ciccotti, H.J.C. Berendsen, Numerical integration of the cartesian equations of motion of a system with constraints: molecular dynamics of n-alkanes, J. Comput. Phys. 23 (3) (1977) 327–341.
[41] A.M. Rydzik, J. Brem, S. Berkel, S. Van, I. Pfeffer, A. Makena, T.D.W. Claridge, C. J. Schofield, Monitoring conformational changes in the NDM-1 metallo- β -lactamase by 19 F NMR spectroscopy, Angew Chem. Int. Ed. Engl. 53 (2014) 3129–3133.
[42] R. Salomon-Ferrer, A.W. Götz, D. Poole, S. Le Grand, R.C. Walker, Routine microsecond molecular dynamics simulations with AMBER on GPUs. 2. Explicit solvent particle Mesh Ewald, J. Chem. Theor. Comput. 9 (2013) 3878–3888.
[43] P.N. Samanta, K.K. Das, Prediction of binding modes and affinities of 4-substituted-2,3,5,6-tetrafluorobenzenesulfonamide inhibitors to the carbonic anhydrase receptor by docking and ONIOM calculations, J. Mol. Graph. Model. 63 (2016) 38–48.
[44] J.M. Seminario, Calculation of intramolecular force fields from second-derivative tensors, Int. J. Quant. Chem. 30 (1996) 1271–1277.
[45] J.J.P. Stewart, Optimization of parameters for semiempirical methods I. Method, J. Comput. Chem. 10 (2) (1989) 209–220.
[46] P.W. Thomas, M. Zheng, S. Wu, H. Guo, D. Liu, D. Xu, W. Fast, Characterization of purified New Delhi metallo- β -lactamase-1, Biochemistry 50 (2011) 10102–10113.
[47] R. Tripathi, N.N. Nair, Mechanism of meropenem hydrolysis by New Delhi metallo β-lactamase, ACS Catal. 5 (2015) 2577–2586.
[48] M.L. Verdonk, J.C. Cole, M.J. Hartshorn, C.W. Murray, R.D. Taylor, Improved protein – ligand docking using GOLD, Proteins: Struct., Funct., Bioinf. 52 (2003) 609–623.
[49] Y.-T. Wang, T.-L. Cheng, Refined models of New Delhi metallo-beta-lactamase-1 with inhibitors: an QM/MM modeling study, J. Biomol. Struct. Dynam. 34 (10) (2016) 2214–2223.
[50] Z. Yu, P. Li, K.M. Merz, Extended zinc AMBER force field (EZAFF), J. Chem. Theor. Comput. 14 (2018) 242–254.
[51] Y. Yu, X. Wang, Y. Gao, Y. Yang, G. Wang, L. Sun, Y. Zhou, X. Niu, Insight into the catalytic hydrolysis mechanism of New Delhi metallo- β - lactamase to aztreonam by molecular modeling, J. Mol. Liq. 282 (2019) 244–250.
[52] Q. Yuan, L. He, H. Ke, A potential substrate binding conformation of β-lactams and insight into the broad spectrum of NDM-1 activity, Antimicrob. Agents Chemother. 56 (10) (2012) 5157–5163.
[53] M. Zheng, D. Xu, New Delhi Metallo-β-lactamase I: substrate binding and catalytic mechanism, J. Phys. Chem. B 117 (2013) 11596–11607.
[54] K. Zhu, J. Lu, F. Ye, L. Jin, X. Kong, Z. Liang, Y. Chen, K. Yu, H. Jiang, J.-Q. Li, C. Luo, Structure-based computational study of the hydrolysis of New Delhi metallo-β-lactmase-1, Biochem. Biophys. Res. Commun. 431 (2013) 2–7.
[55] R. Zwanzig, Nonlinear generalized Langevin equations, J. Stat. Phys. 9 (3) (1973) 215–220.